# Turbulent cascades in anisotropic magnetohydrodynamics

R. M. Kinney and J. C. McWilliams
*Institute of Geophysics and Planetary Physics, University of California at Los Angeles, Los Angeles, California 90024*
*and National Center for Atmospheric Research, Boulder, Colorado 80307*
(Received 17 December 1997)

The cascade behavior of turbulent magnetohydrodynamics with a strong background magnetic field is examined and compared with direct numerical solutions at high Reynolds number. Resonant interactions give rise to qualitatively different behavior for modes below a characteristic wave number $k_L$ defined in terms of the background field. Modes with parallel wave number above $k_L$ are passively driven by the longer wavelength modes, even when the majority of the energy is contained in the passive wave numbers. The passive modes do not cascade to higher parallel wave numbers, so the parallel wave number spectrum is not a power law and does not extend to dissipation scales. Energy is cascaded normally to small perpendicular scales, but more rapidly in the case of the passive modes, so an anisotropic spectrum develops from isotropic initial conditions. For a finite system with minimum wave number $>k_L$, the only dynamically controlling mode is the vertical average, or mean mode. The mean mode evolves with two-dimensional dynamics, forming coherent current structures which are mirrored by the passive modes. Because of the differential decay rates, the mean mode dominates at long times. Quantitative comparisons are made to numerical solutions of reduced magnetohydrodynamics. [S1063-651X(98)06406-X]

PACS number(s): 52.35.Ra, 47.65.+a, 52.65.Kj

## I. INTRODUCTION

Although theoretical studies of turbulence usually begin with assumptions of homogeneity and isotropy, such assumptions are more often motivated by convenience than physical arguments. In a plasma, isotropy is particularly difficult to justify, for nearly every naturally occurring plasma, from terrestrial to solar to galactic scales, possesses a magnetic field on the largest scale of the system. Laboratory plasmas are also usually constructed with large-scale magnetic fields necessary for confinement. The theory of turbulent magnetohydrodynamics (MHD) in the presence of a large-scale magnetic field is in need of further development.

Observations and laboratory measurements reveal that turbulent fluctuations against a strong background field tend to have longer length scales along the field direction and that the fluctuating component in the direction of the field is smaller than the components perpendicular to the field. These conclusions have been drawn by scintillation observations of distant objects viewed through the interstellar magnetic field [1] or near the solar limb [2], or from direct measurement of the fluctuations via spacecraft in the solar wind [3–5], and have also been noted in tokamak experiments [6]. Some of these features have also been seen in numerical solutions of three-dimensional (3D) MHD. Spectral anisotropy was found from isotropic initial conditions in incompressible MHD [7], while anisotropy in the magnetic field vector components was found in compressible solutions [8]. The degree of anisotropy in the fluctuations was observed to increase with the strength of the background field, but the dynamical mechanism by which these anisotropies develop is still not well understood, and large Reynolds numbers are still not achievable in 3D MHD solutions.

Although classical MHD turbulence theory is nominally isotropic, closure calculations [9] assign a key role to magnetic helicity, an inherently anisotropic quantity. Furthermore, in inertial-range scaling arguments [10,11], a large-scale magnetic field is presumed to influence the small scales by the ''Alfvèn effect,'' in which the small-scale fluctuations ''see'' a large-scale magnetic field as a constant background and thus behave like Alfvén waves. Classically, the effect of the large-scale field is simply to reduce the mode interaction time when determining the isotropic inertial-range spectrum. However, the interaction of Alfvén waves is unusual in that waves traveling in the same direction do not interact at all (barring compressible and dissipative effects). Thus it has been argued that the three-wave interactions are in fact empty unless one of the modes in the triad has zero component along the mean magnetic field [12,13], and that energy is therefore more efficiently transferred to perpendicular wave numbers. It has also been argued [14] that such modes, by virtue of having zero frequency, do not contribute at all to the interactions, and that the cascade is therefore determined by the four-wave resonant interactions [15]. Direct numerical tests of the interaction between pairs of wave packets have shown that the triad interactions do dominate [18], but it has been claimed that in a fully turbulent state with many interacting packets, all orders will contribute equally [19].

Reduced MHD (RMHD) [20,21] is a reduction of MHD with three spatial dimensions and two-dimensional (2D) field components. It was originally derived for tokamak fusion devices from scaling arguments based on a strong vertical magnetic field. In fact, environmental anisotropies other than background magnetic fields (such as strong rotation) can lead to dynamics closely related to RMHD [22]. The dynamics of the time-dependent parallel components (which have no influence on the perpendicular component evolution) differ under different scalings [22]. RMHD was used to compute the triad interactions in Ref. [18], and the restriction to consideration of shear Alfvén waves in Refs. [14,15] is in fact

 

equivalent to starting from RMHD. Although a simplification, RMHD is advantageous in that its solutions are far easier to compute than MHD, making possible studies at higher Reynolds number. RMHD has all of the important dynamical features relevant to the development of anisotropy in MHD: three dimensionality, cascade behavior in all directions, and a competition between linear and nonlinear forces.

In this paper we present an analysis of the effects of a strong background magnetic field on turbulent MHD. Section II explores the effects of a strong background field when a range of parallel scales is present. In a multiple-time-scale analysis, the behavior of both the slowly varying components and the slow WKB behavior of the rapidly varying components are derived. The analysis is carried out for RMHD, and the generalization to 3D incompressible MHD is given in the Appendix. Section III gives results from high-resolution long-time integrations of RMHD which confirm the predictions of Sec. II. Section IV gives our conclusions.

## II. MULTIPLE TIME SCALES OF ANISOTROPIC MAGNETOHYDRODYNAMICS

Plasmas contain motions on an enormous range of time scales. MHD is itself a simplification of the basic plasma equations in which certain fast-time scales (e.g., particle gyrofrequency, plasma frequency) have been removed, yet even MHD has a multiplicity of time scales, and further reductions are useful to make analysis less difficult. Here, we study RMHD, in which fast compressional modes are absent, but shear Alfvén waves remain. It should be emphasized that our analysis can be equally well applied to 3D incompressible MHD, as is presented in the Appendix. The fundamental dynamical consequences of the analysis are the same for both systems. The RMHD analysis is emphasized in the text so that we may make explicit comparisons with numerical solutions.

We adopt a notation in which boldface denotes purely horizontal vector components. Likewise, $\boldsymbol{\nabla}$ is the perpendicular gradient and $\nabla^2$ is the perpendicular Laplacian $\partial_x^2 + \partial_y^2$. The magnetic field is measured in units of velocity, there is a constant vertical magnetic field $B_0$, and the density is assumed constant. In terms of scalar potentials $\psi$, $A$, the perpendicular velocity is given by $\mathbf{v}=\hat{\mathbf{z}}\times\boldsymbol{\nabla}\psi$ and the perpendicular magnetic field by $\mathbf{B}=\hat{\mathbf{z}}\times\boldsymbol{\nabla}A$. The RMHD equations,

$$\partial_t\zeta+[\psi,\zeta]-[A,j]=B_0\partial_z j, \tag{1a}$$

$$\partial_t A+[\psi,A]=B_0\partial_z\psi, \tag{1b}$$

determine the evolution of the perpendicular components of the fields, where $\zeta=\nabla^2\psi$ is the parallel vorticity, $j=\nabla^2 A$ is the parallel current, and $[\cdot,\cdot]$ is the horizontal Jacobian. The parallel components of the velocity and magnetic fields are passively driven by the $\psi$ and $A$ fields. Introducing the Elsasser fields $\mathbf{u}^\pm=\mathbf{v}\pm\mathbf{B}$, $\psi^\pm=\psi\pm A$, and $\Omega^\pm=\nabla^2\psi^\pm$, RMHD can also be written by taking the sum and difference of Eq. (1a) and the Laplacian of Eq. (1b),

$$\partial_t\Omega^\pm+\boldsymbol{\nabla}\cdot[\psi^\mp,\boldsymbol{\nabla}\psi^\pm]=\pm B_0\partial_z\Omega^\pm. \tag{2}$$

Neglecting boundary sources, RMHD has three integral invariants,

$$\int |\boldsymbol{\nabla}\psi^+|^2+|\boldsymbol{\nabla}\psi^-|^2 d\mathbf{x}dz, \quad \int |\boldsymbol{\nabla}\psi^+|^2-|\boldsymbol{\nabla}\psi^-|^2 d\mathbf{x}dz,$$

$$\int A d\mathbf{x}dz, \tag{3}$$

which are the total energy, cross-helicity, and magnetic helicity. These invariants are the same as general 3D MHD, whereas in 2D, the magnetic helicity invariant is replaced by the $\int A^2 d\mathbf{x}$.

The resonant interaction of MHD waves has been known for some time [16], and can be stated in terms of the formal theory of partial differential equations [17]. For a small parameter $\epsilon\ll 1$, if the terms in Eq. (2) containing $B_0$ are larger by $1/\epsilon$ than the nonlinear terms, one can postulate a fast-time scale $t'$ and a slow-time scale $\tau$ such that $\partial_t=(1/\epsilon)\partial_{t'}+\partial_\tau$ and $\psi^\pm=\psi^\pm(\mathbf{x},z,t',\tau)$. The fast-time-scale behavior is determined by the $O(\epsilon^{-1})$ parts of Eq. (2) and the slow response by the $O(1)$ parts. The multiple time scale is distinct from a simple asymptotic expansion in $\epsilon$. Applying the analysis to 3D MHD, one finds that the slow-time-scale behavior is given by 2D MHD [23], while RMHD follows by additionally assuming fast and slow variations in $z$ [21,24].

Applying resonance theory to broadband turbulence requires some care. In truth, a simple scaling in which the $B_0$ term in Eq. (2) is larger by $1/\epsilon$ than the nonlinear term is overly simplistic, since the size of the linear term depends on the strength of the $z$ derivatives and a large range of scales may be present. To account for all possible parallel scales, we introduce the vertical Fourier transform of $\Omega^\pm$,

$$\Omega^\pm=\sum_k \Omega_k(\mathbf{x},t)e^{ikz}, \tag{4}$$

and write Eq. (2) as

$$\partial_t\Omega_k^\pm=-\boldsymbol{\nabla}\cdot\sum_{k'}[\psi_{k'}^\mp,\boldsymbol{\nabla}\psi_{k-k'}^\pm]\pm ikB_0\Omega_k^\pm. \tag{5}$$

If the typical perpendicular scale and amplitude of all $\psi_k^\pm$ modes are comparable, then the question of whether the linear term dominates over the nonlinear term is dependent on the value of $k$. Let us define a cutoff wave number for linear behavior, $k_L$, such that modes for which $k\ll k_L$ evolve mostly via the nonlinearity, while those for which $k\gg k_L$ evolve mostly linearly. An estimate for $k_L$ is

$$k_L\sim\frac{\overline{\kappa v}}{B_0}, \tag{6}$$

for a characteristic perpendicular wave number $\overline{\kappa}$ and perpendicular velocity $\overline{v}$. The behavior of the system depends on the scale content relative to $k_L$. Below we consider three different cases for initial excitations with wave number $k_0$.

### A. $k_0 \gg k_L$

One possibility is that all finite wave numbers present in the initial conditions are $>k_L$. In a finite system with a minimum wave number, one may have $k_L$ less than the minimum wave number, but there may still be energy in the $k=0$ mode. The fast-time-scale behavior is given by the $O(\epsilon^{-1})$ part of Eq. (5),

$$\partial_{t'}\Omega_k^{\pm} = \pm ikB_0\Omega_k^{\pm}, \tag{7}$$

so that

$$\Omega_k^{\pm} = \Omega_k(\mathbf{x},\tau)e^{\pm ikB_0t'} \tag{8}$$

for all $k$, including $k=0$ which does not evolve on the fast-time scale. The fast-time behavior is nondispersive Alfvén wave propagation with speed $B_0$ either parallel (for $\Omega^-$) or antiparallel (for $\Omega^+$) to the background magnetic field. Obviously, there is no transfer among wave numbers on the fast time scale. We may calculate the $O(1)$ parts of Eq. (5),

$$\partial_\tau\Omega_k^{\pm}e^{\pm ikB_0t'} = -\boldsymbol{\nabla}\cdot\sum_{k'}[\psi_{k'}^{\mp},\boldsymbol{\nabla}\psi_{k-k'}^{\pm}]e^{\pm i(k-2k')B_0t'} \tag{9}$$

and isolate the slow-time behavior by projection (i.e., multiplying by $e^{\mp ikB_0t'}$ and averaging over the fast phase variations). The time averaging of the nonlinear terms gives rise to a cancellation of the interaction between most Fourier modes, i.e., in the summation over $k'$, only the terms with $k'=0$ survive. This is a peculiarity of shear Alfvén waves in ideal MHD, and comes from the fact that waves traveling in the same direction do not interact at all [12]. This resonance condition breaks down when nonideal effects are considered, such as compressibility or unequal viscosity and resistivities. The result of the averaging is

$$\partial_\tau\Omega_k^{\pm} + \boldsymbol{\nabla}\cdot[\psi_0^{\mp},\boldsymbol{\nabla}\psi_k^{\pm}] = 0, \tag{10}$$

which describes the slow WKB evolution of Alfvén wave amplitudes.

Inspection of Eq. (10) shows that the $k=0$ mode evolves independently of all the finite-$k$ modes. Furthermore, the dynamics of the $k=0$ mode (which we refer to as the ''mean mode'') are just those of 2D MHD. That the mean mode can be associated with the slow-time-scale dynamics of anisotropic MHD has been known for some time [23]. An important point is that the plasma need not be weakly $z$ dependent; the independence of the mean mode arises from the short interaction time of oppositely propagating waves. In effect, the only $(x,y,t)$ field affecting a propagating wave is that of the mean mode, whose presence is felt continuously.

Each of the finite-$k$ components (the ''wave modes'') has a separate subdynamics which are driven by the mean mode without influencing it. An additional consequence of Eq. (10) is that

$$\partial_\tau\int|\boldsymbol{\nabla}\psi_k^{\pm}|^2d\mathbf{x} = 0, \tag{11}$$

i.e., the energy in each wave mode is conserved individually. Thus there is no cascade in parallel wave number on the slow-time scale either. Any transfer of energy among different $k$ must be through higher-order interactions. In the perpendicular directions, however, there is a cascade on the slow-time scale which is entirely controlled by the mean mode. Because the mean mode will undergo the forward energy cascade characteristic of 2D MHD, the wave modes will also be driven to small perpendicular wavelengths on the slow-time scale. However, the time scale of this cascade is controlled by the amount of energy in the mean mode and if the mean mode is very weak, the cascade may instead be controlled by higher-order effects neglected here. The passive behavior of the high-$k$ modes holds for 3D MHD as well as RMHD (see the Appendix).

It has been speculated previously that the more rapidly varying components would evolve ''parasitically'' to the slowly varying component in anisotropic MHD [23]. Triad interactions between individual wave packets have been explicitly calculated and verified numerically [18], but may not dominate over many collisions [19]. Equation (10) is appropriate to broadband turbulence and will be compared directly against the behavior of 3D RMHD numerical solutions below.

### B. $k_0 \ll k_L$

If the initial excitation is at wave numbers less than the linear cutoff $k_L$, then the primary dynamics are nonlinear. In this case, the interaction time between wave packets is long enough that they may interact without being resonant and we expect a turbulent cascade to higher wave numbers by the usual doubling in wave number space, i.e.,

$$\partial_t\Omega_{2k}^{\pm} \sim \Omega_k^{\mp}\Omega_k^{\pm} + 2ikB_0\Omega_{2k}^{\pm}. \tag{12}$$

Although initially unexcited modes grow in amplitude due to nonlinear coupling from lower-$k$ modes, this is not a cascade in the traditional sense because of the characteristic amplitude $B_0$. We can presume based on the preceding subsection that if a mode $\Omega_{2k}$ grows to an amplitude such that the linear term in Eq. (12) is approximately as strong as the nonlinear term, the mode will begin to interact only in resonant triads (i.e., will be passively driven by the mean mode), and will no longer cascade to higher wave numbers. Thus the extent of the cascade in $k$ is limited not by dissipation, but by the background field $B_0$. A mode will grow in amplitude until there is an approximate balance between the terms in Eq. (12). This implies a parallel spectrum with $\Omega_{2k}\sim\Omega_k^2$, which suggests an exponential form $\Omega_k\sim e^{ak}$. On dimensional grounds, the natural choice for the exponential scale factor is $k_L$, giving a parallel spectrum

$$\Omega_k^{\pm} \sim e^{-|k/k_L|}. \tag{13}$$

If $k_L$ is small ($B_0$ large), the turbulent cascade will be strongly suppressed before reaching dissipation scales. Higher-order effects may still give rise to significant transfer of energy to small scales, so nonlinear numerical solutions are necessary to verify the inhibition of cascade.

The value of $k_L$ depends on the characteristic perpendicular wave number $\kappa$, which may increase when the initial excitation undergoes a perpendicular cascade. It has been suggested [15] that a scale-invariant cascade occurs such that

the mean parallel wave number $\overline{k}$ increases at the same rate as $k_L$. We must establish whether the increase in $k_L$ interferes with the scaling argument leading to the above exponential spectrum.

Suppose the perpendicular energy cascade of an excitation with initially isotropic wave number $k_0$ leads to a developed perpendicular spectrum

$$E_\kappa \sim \frac{v_0^2}{k_0}\left(\frac{\kappa}{k_0}\right)^{-n}, \tag{14}$$

up to some dissipation cutoff $\kappa_d \gg k_0$. If the energy is to be finite and the energy dissipation rate independent of the viscosity, then $1<n<2$. The characteristic entropy can be estimated by

$$\overline{\kappa^2}\overline{v^2} \sim \int \kappa^2 E_\kappa d\kappa. \tag{15}$$

After the spectrum has fully developed, $k_L$ as estimated by Eq. (6) will have increased from its initial value to

$$k_L \sim \kappa_d \frac{v_0}{B_0}\left(\frac{\kappa_d}{k_0}\right)^{(1-n)/2}. \tag{16}$$

Although much larger than its initial value, $k_0 v_0/B_0$, the final value of $k_L$ is still $\ll \kappa_d$. Therefore the parallel spectrum will always be dominated by the exponential dependence in Eq. (13) rather than by the power law of a scale-invariant cascade to dissipation. (Note, however, that if collisions are infrequent, the viscous operator in a plasma is anisotropic [26]. Since the parallel dissipation wave number $k_d$ is then $\ll \kappa_d$, a short inertial range might be established instead of an exponential spectrum.)

Our conclusion is that the standard picture of a scale-invariant Kolmogorov-type cascade does not apply in the direction parallel to a strong magnetic field. There is a fundamental difference in energy transfer rates at different parallel scales because large-$k$ modes that are excited soon become oscillatory and decouple from the rest of the system. In particular, this stops the cascade from progressing to dissipation scales in the parallel wave number and implies an exponential spectrum rather than the traditional power law.

### C. $k_0 \sim k_L$

If the initial excitation contains wave numbers across a large range, a quantitative assessment is difficult. We can expect that those wave numbers $\gg k_L$ will decouple from the smaller-$k$ modes and evolve according to the resonant interactions in Sec. II A, effectively truncating the parallel spectrum at wave number $k_L$. However, the mean mode will not evolve independently with 2D dynamics, as in the resonant case. Instead, all modes with $k<k_L$ will be coupled to form a dynamical system whose evolution is independent of the $k \gg k_L$ modes.

## III. NUMERICAL SOLUTIONS OF TURBULENT RMHD

We test the results of the multiple-time-scale analysis by numerically calculating solutions of RMHD in the form given by Eq. (1). The numerical scheme is finite difference, with the nonlinear terms calculated by discretization of the Jacobian operator, for which several second- and fourth-order symmetric algorithms were tested. The elliptic problem for the vorticity-streamfunction diagnostic equation (i.e., solving $\zeta = \nabla^2 \psi$ for $\psi$) is solved by an iterative multigrid algorithm discretized with a second-order operator which is based on staggered differences, giving it an effective cutoff scale compatible with the higher-order advection schemes. A staggered vertical grid is used, with $\psi$ and $A$ defined on conjugate grids and either second- or fourth-order schemes used to evaluate vertical derivatives. In combination with a centered leapfrog time stepping, this has the implication that vertical Alfvén waves are not dissipated by the numerical method, which is important when investigating questions of spectral transfer in the parallel. We use a purely horizontal dissipation operator so that energy is explicitly removed at small horizontal scales with no such sink for wave vectors parallel to $\hat{\mathbf{z}}$. Various dissipation operators are used, including the commonly used hyperdiffusion $-\nu\nabla^4$ and a nonlinear variant of this (i.e., the $\gamma$ scheme of Ref. [27]), which allow a somewhat larger inertial range and narrower dissipation range compared with ordinary diffusion. Although the choice between higher-order finite difference schemes can affect the outcome of sensitively dependent deterministic problems and can influence the late-time shape of coherent structures [27], we find that our results do not change appreciably under different numerical schemes. In particular, none of the results we quote are sensitive to choice of dissipation operator.

We define the parallel mode energies

$$E_k = \int |\nabla \psi_k|^2 + |\nabla A_k|^2 d\mathbf{x}, \tag{17}$$

such that the total energy is $\Sigma_k E_k$. Similarly, we define the horizontal Fourier transforms,

$$\hat{\psi}(\kappa, z) = \int \psi e^{i\kappa\cdot\mathbf{x}} d\mathbf{x}, \tag{18}$$

and the energies

$$\hat{E}_\kappa = \sum_{|\kappa'|=\kappa} \kappa'^2 \int |\hat{\psi}(\kappa', z)|^2 + |\hat{A}(\kappa', z)|^2 dz, \tag{19}$$

so that the total energy is $\Sigma_\kappa \hat{E}_\kappa$. The mean parallel and perpendicular wave numbers are measured by

$$\overline{k^2} \equiv \frac{\sum_k k^2 E_k}{\sum_k E_k}, \quad \overline{\kappa^2} \equiv \frac{\sum_\kappa \kappa^2 \hat{E}}{\sum_\kappa \hat{E}}. \tag{20}$$

The normalization is such that the computational domain is a cube with edge length $2\pi$ and $\int |\nabla \psi|^2 + |\nabla A|^2 d\mathbf{x} dz = 1$ at $t = 0$. In this paper we discuss only unforced solutions, so the energy is a decaying function of time. We adopt a normalization in which "$B_0 = 1$" means that $\int B_0^2 d\mathbf{x} dz = 1$. Thus a vertical Alfvén transit time for $B_0 = 1$ is approximately $\Delta t = 100$. The initial spectrum is chosen with random phases

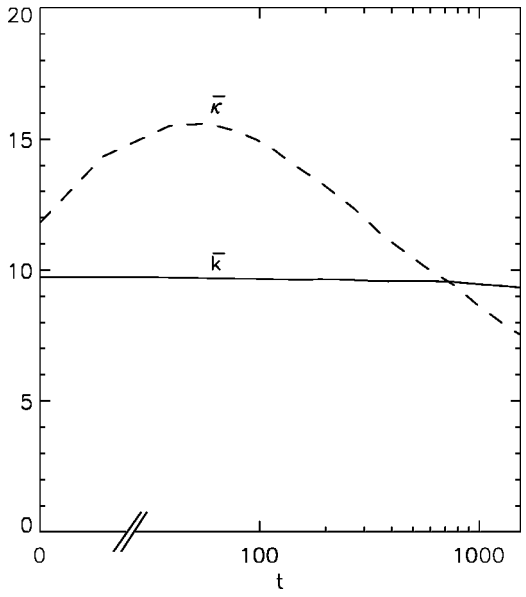


FIG. 1. Parallel wave number moment $\bar{k}$ (solid) and perpendicular moment $\bar{\kappa}$ (dashed) from decaying RMHD solution with $B_0=5$. The parallel wave number shows almost no evolution, while the perpendicular wave number shows a normal cascade.

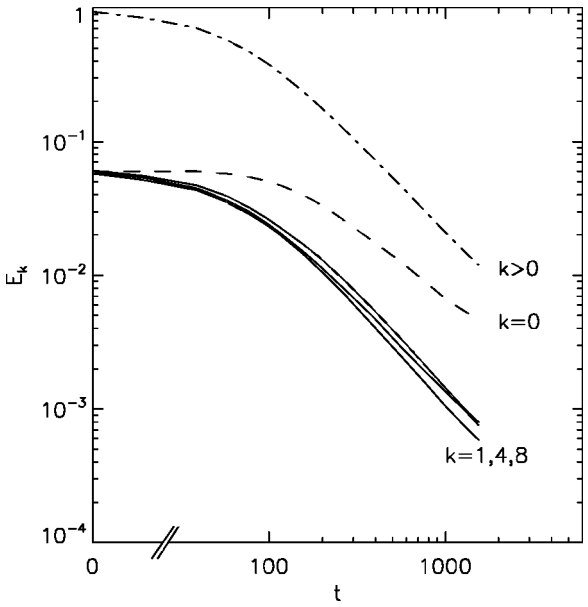


FIG. 2. Evolution of energy contained in various modes. The $k=0$ mode decays more slowly than the finite-$k$ modes and will eventually dominate the solution.

such that $\hat{E}_\kappa$ is peaked at $\bar{\kappa}=5$ and $E_k$ is constant for $k$ between 0 and a finite $k_{\max}$, typically $\frac{1}{8}$ of the maximum resolved wave number.

### A. Strong background field

We begin by examining solutions with $B_0$ large, in which case the dominant interaction is expected to be the resonant dynamics of Eq. (10). By Eq. (6), choosing $B_0=5$ gives $k_L=2$, so that all the modes should obey Eq. (10), with no interaction between different parallel modes. Figure 1 shows the mean parallel and perpendicular wave numbers vs time in a $B_0=5$ solution calculated on a $128^3$ grid. No parallel cascade is evident, but a cascade proceeds normally in the perpendicular wave numbers. While $\bar{k}$ remains constant to within 2% during the entire solution, $\bar{\kappa}$ increases as the spectrum broadens, with a maximum at $t\approx 60$. After reaching its maximum, $\bar{\kappa}$ decays due to dissipation and the absence of forcing.

In the absence of a parallel cascade, all energy dissipation occurs via cascade to small perpendicular scales. Since the

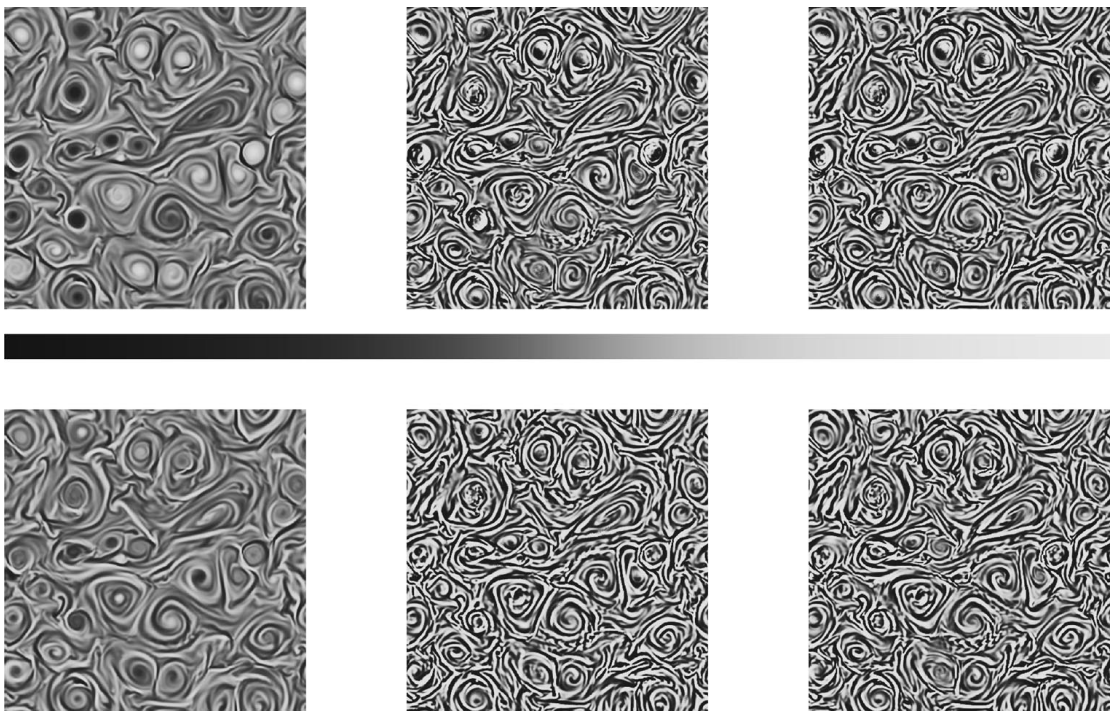

FIG. 3. On the left are visualizations of the current (top) and vorticity (bottom) of the mean mode of a $512^2\times 32$ solution at $t=1100$. In the middle are the time derivatives of the fields. On the right are what the time derivatives would be for a 2D solution.

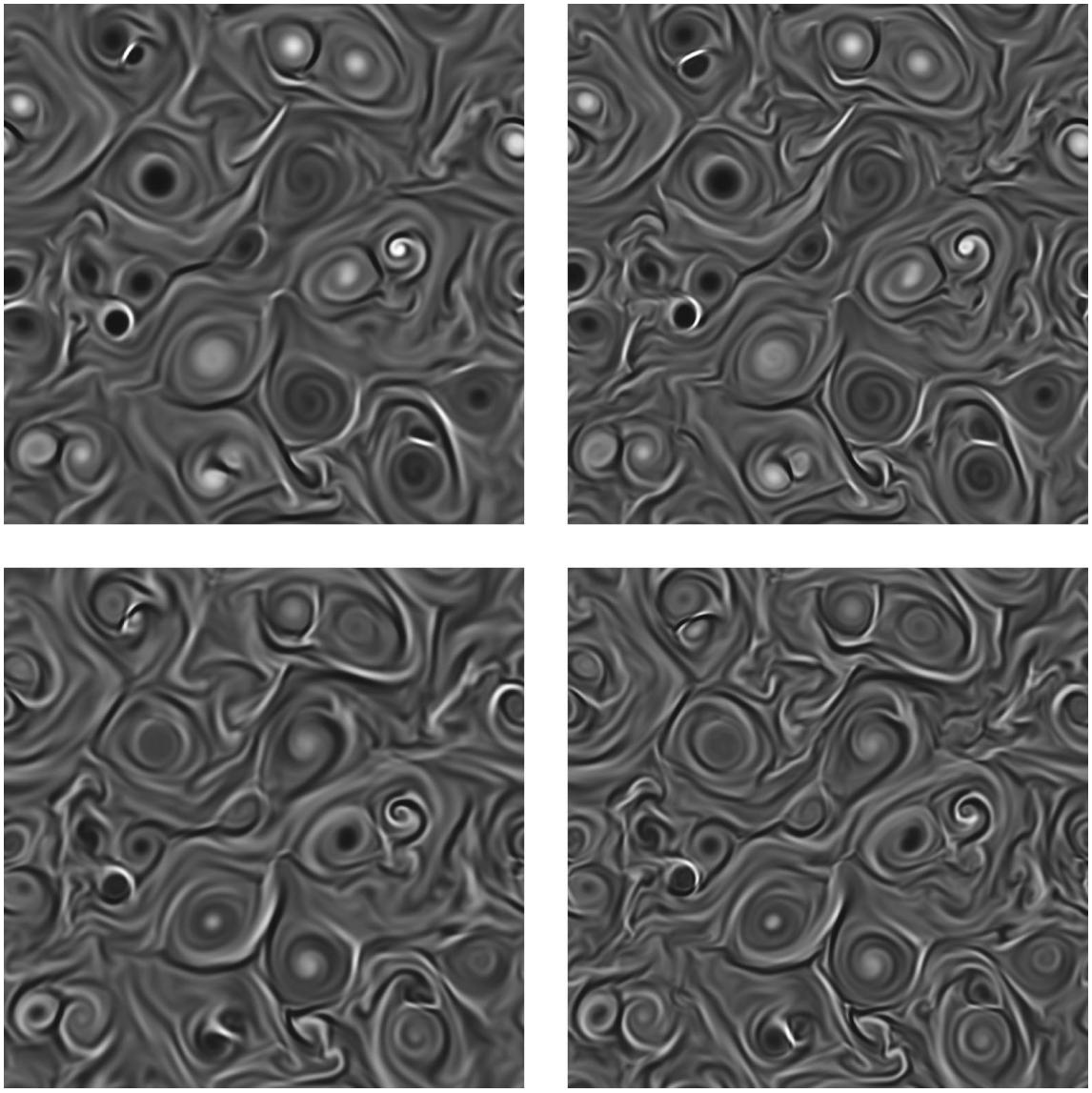

FIG. 4. Current (above) and vorticity (below) of the mean mode of a 3D solution on the left and a 2D solution initialized with the fields in Fig. 4, showing persistence of 2D dynamics in the 3D case over many decorrelation times.

mean mode is the only one with nonlinear dynamics, its behavior is fundamentally different from the other modes. All of the wave modes should behave similarly since our computational method dissipates all parallel modes equally. Figure 2 shows $E_k$ as a function of time for various $k$. The numerical value of the decay rates should converge with large Reynolds number. Although we cannot establish that the measured rates are universal, a clear difference between the mean and wave modes is visible. The energy of the mean mode $E_0$, decays more slowly than the others. The sum of all modes with $k>0$ is also shown. In this solution, the mean mode begins with 6% of the total energy and ends with 40%. The $t\to\infty$ state is clearly one in which the mean mode will dominate all other modes.

The dynamics of the mean mode are plainly those of 2D MHD. Rigorous attributes such as conservation of $\int A_0^2 d\mathbf{x}$ are observed along with phenomenological features reported in previous solutions of 2D turbulent MHD (e.g., Ref. [25]) such as dominance of magnetic over kinetic energy throughout the spectrum and rising current kurtosis [25]. Visualizations of the mean mode amplitudes of current $j_0(\mathbf{x})$ and vorticity $\zeta_0(\mathbf{x})$ are shown on the left hand side of Fig. 3. The time shown is $t=1130$ in a $B_0=5$ solution on a $512^2 \times 32$ grid. The fields have very similar appearance to those from 2D solutions, with magnetic vortex structures and thin current and vorticity sheets [25]. In the middle are $\partial_\tau j_0$ and $\partial_\tau \Omega_0$ from the 3D solution, calculated from the difference in the fields at two nearby times. On the right is the result obtained by calculating what the time derivatives would be for 2D dynamics. The time evolution of the mean mode is very closely predicted by the simple 2D dynamics. The correlation coefficient for the two fields (defined for two functions $g$ and $h$ as $\int gh/\sqrt{\int g^2 \int h^2}$) is 0.74, with the difference most probably due to the fast-time-scale forcing present in the 3D solution. These dynamics persist over long times. Figure 4 shows the current and vorticity of the mean mode at $t=1660$ on the left, compared with the fields from a 2D solution initialized with the mean mode field at $t=1130$. The

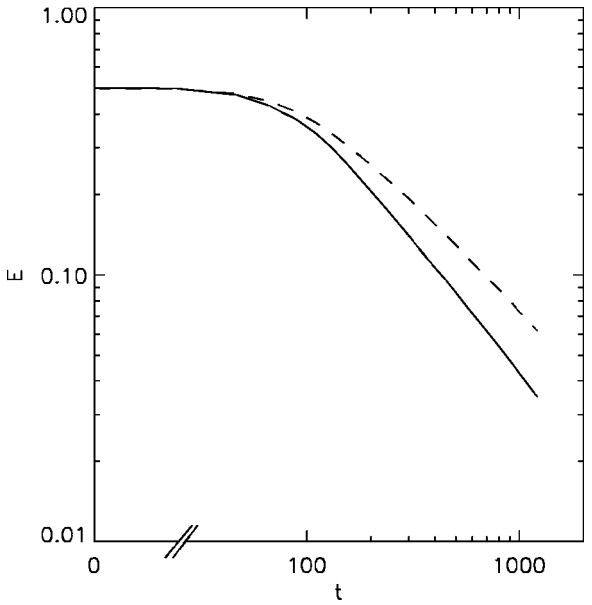


FIG. 5. Energy of decaying 2D MHD solution (dashed line) and a passive field driven according to Eq. (10) (solid line). The difference in decay rates is similar to what is observed in Fig. 2.

time elapsed is greater than a decorrelation time (correlation coefficients between the 3D fields at the initial and final times are 0.025 and 0.003 for the current and vorticity, respectively), but the 2D and 3D solutions are still well correlated (coefficients 0.69 and 0.65). Correlations over longer times should decrease because of the sensitive dependence on initial conditions inherent to these equations.

The slower decay rate of the dynamical fields is attributable the development of the coherent structures apparent in Fig. 4. A similar mechanism occurs in 2D neutral fluid turbulence, in which the entropy decays more slowly than the variance of a passive scalar because the coherent structures formed in the vorticity field inhibit the cascade to dissipation [28]. Figure 5 shows the results of a 2D MHD calculation in which the evolution of a passive field was evolved according to Eq. (10) simultaneously with the MHD fields. The passive field decays at a faster rate than the dynamical fields. The 2D solution shown in Fig. 5 is at higher Reynolds number than the 3D solution of Fig. 2; 2D solutions with the same Reynolds number as the 3D solution shown in Fig. 5 have similar values for the power-law decay rates.

A consequence of the passive dynamics of Eq. (10) is that the wave mode amplitudes $\Omega^{\pm}_{k>0}$ acquire horizontal structure from the mean mode. The form of passive interaction in Eq. (10) is different from a simple passive scalar; the quadratic invariant is an energy rather than a scalar variance (here enstrophy, $\int|\Omega^{\pm}_{k}|^2 d\mathbf{x}$). The mean mode has a direct cascade of energy and evolves coherent structures. The wave modes develop a similar perpendicular spectrum and exhibit ghost structures. On the left in Fig. 6 is the mode amplitude $|\Omega^{+}_{2}|^2$ from the $512^2\times 32$ RMHD solution at $t=1660$, the same time as shown in Fig. 4. It is clear that the $\Omega^{+}_{2}$ cross section mirrors certain vortex features apparent in $j_0$. On the right is the result of a 2D integration of Eq. (10), starting from initial conditions given by the $\Omega^{+}_{2}$ mode at $t=1130$, i.e., the fields in Fig. 3. The correlation coefficient between the fields given by the 3D and 2D solutions is 0.87, demonstrating the long-term applicability of Eq. (10) over many decorrelation times.

It should be emphasized that the validity of 2D dynamics for the mean mode of a 3D solution does not depend on the mean mode being energetically dominant. The dynamics come about purely for reasons of multiple time scales. For example, in Fig. 2, the mean mode comprises less than half of the total energy. The fraction of energy contained in the mean mode grows because of the difference in decay rates, but the dynamics of the mean mode are 2D long before it dominates energetically. Visualizations in 3D of subdomains containing current structures are shown in Fig. 7. The mean mode is not dominant in the case on the left. While it is

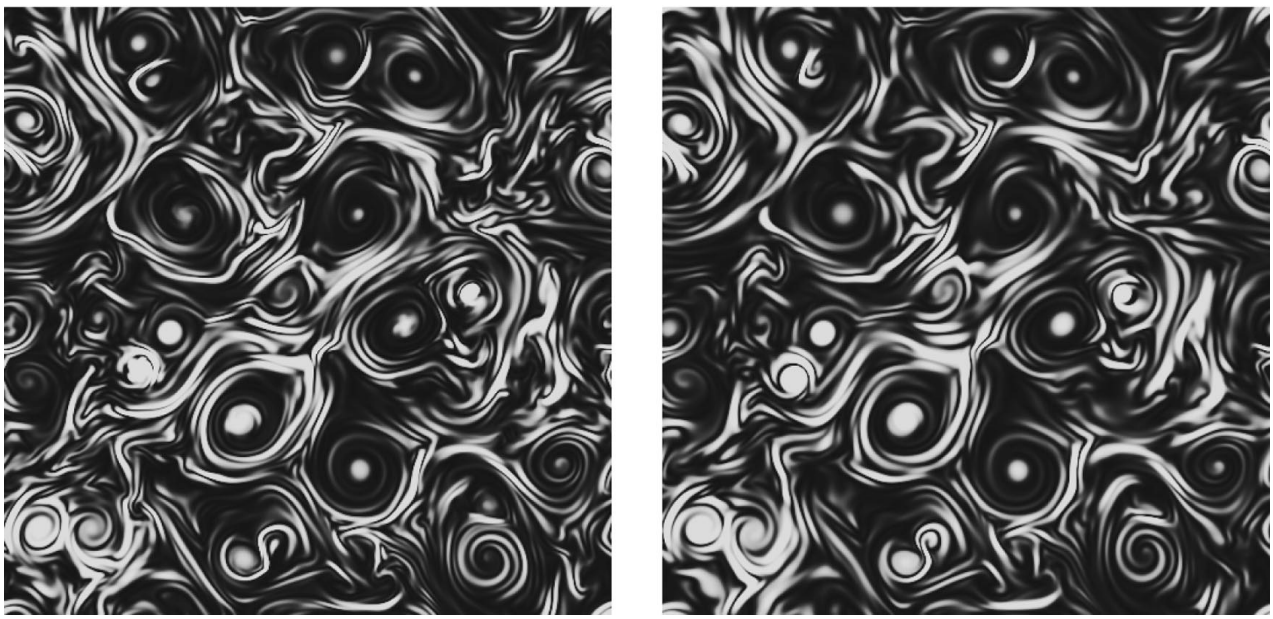

FIG. 6. Amplitude of the $\Omega^{+}_{k=2}$ mode from a 3D solution at $t=1660$ (left) compared with a 2D calculation initialized from the fields at the time shown in Fig. 3. Passive driving of the wave modes by the mean mode is consistent over many decorrelation times.

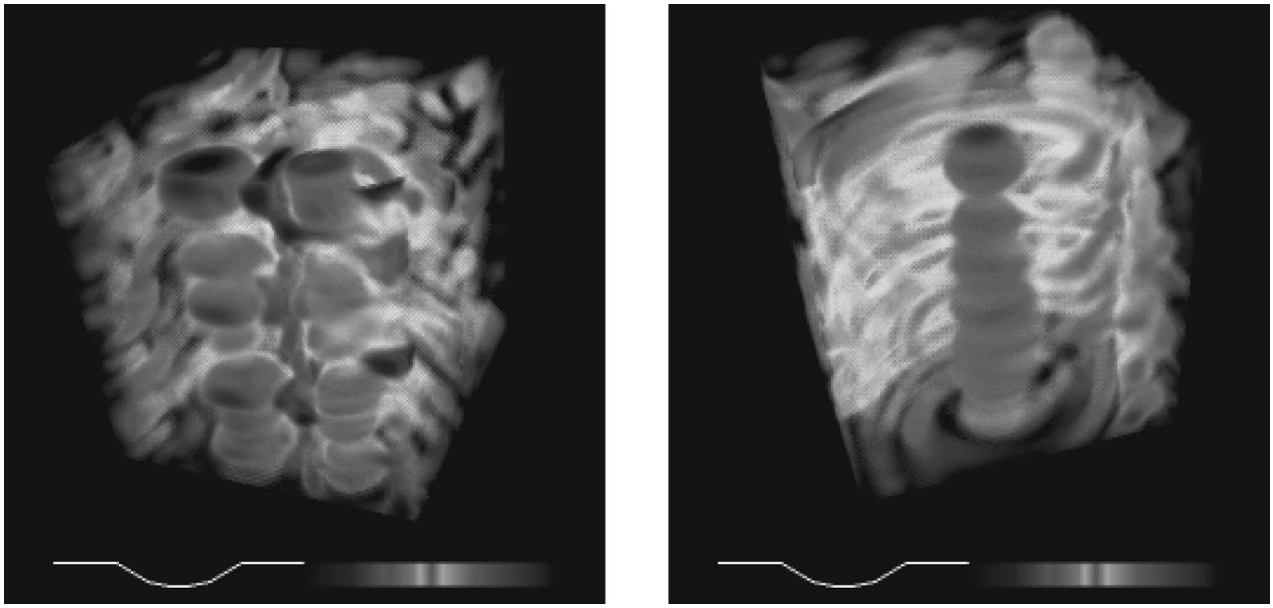

FIG. 7. Details of coherent structures in the parallel current of 3D RMHD solutions. Structures occur whether the $k=0$ mode has comparable energy with the finite-$k$ modes (left) or is dominant (right).

possible to see that the vertically averaged current is structured, the total current can even reverse sign at particular levels, a result of beating by the wave modes. The right hand case is one in which the mean mode is dominant and the structures appear more vertically uniform.

### B. Moderate background field

Although we do not present a higher-order theory in this paper, we can observe the effects of higher-order interactions not considered in deriving Eq. (10) by calculating solutions with $B_0<1$. Although RMHD is derived based on physical arguments of a ''strong'' background magnetic field, RMHD is well behaved for small $B_0$ since $B_0$ appears only in combination with $\partial_z$. Choosing $B_0$ small in Eq. (1) should be interpreted as a rescaling of the vertical coordinate, as arising from a scale anisotropy in the initial conditions. The physical picture of taking the $B_0\to 0$ limit of Eq. (1) is a collection of packets far removed in $z$ but still linked by a strong magnetic field. The extreme of this limit yields a system of independently evolving 2D planes, which while physically meaningful, is clearly distinct from 3D MHD in the absence of a background magnetic field. The independent evolution of the horizontal planes leads to the generation of parallel gradients

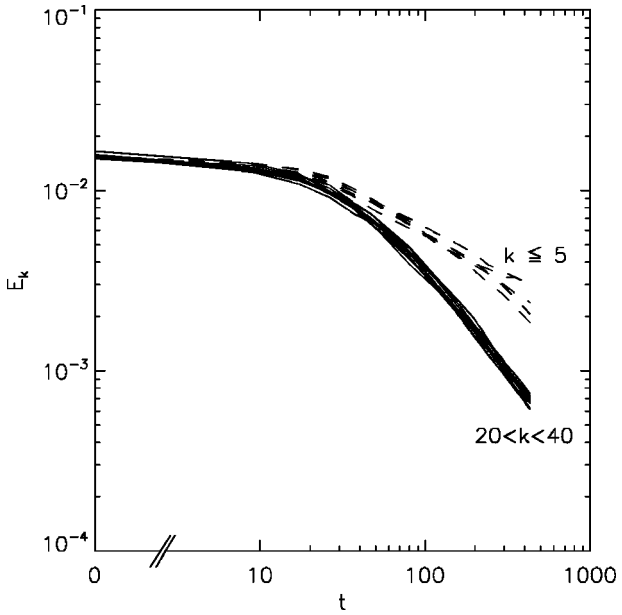


FIG. 8. Energy of selected modes vs time for $B_0=0.2$ solution. The small-$k$ modes decay at a markedly slower rate than the high-$k$ modes, analogous to the situation in Fig. 2.

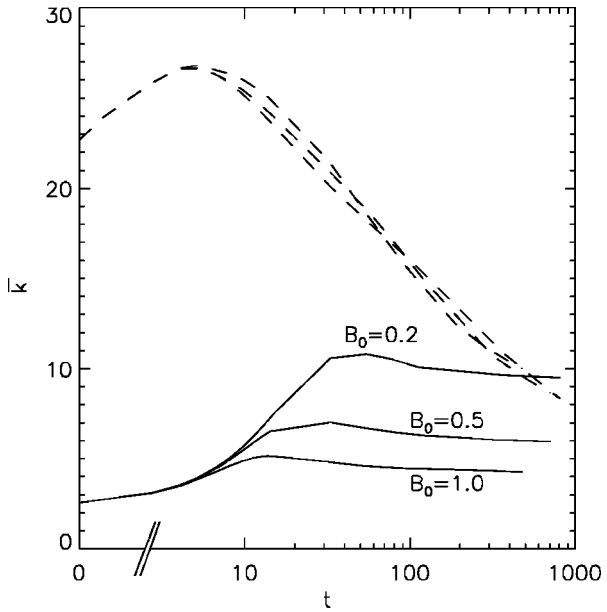


FIG. 9. Parallel (solid) and perpendicular (dashed) wave number moments for three solutions with different $B_0\leqslant 1$. The parallel cascade is limited by the magnetic field strength rather than by dissipation, while the perpendicular cascade is unaffected by magnetic field strength.

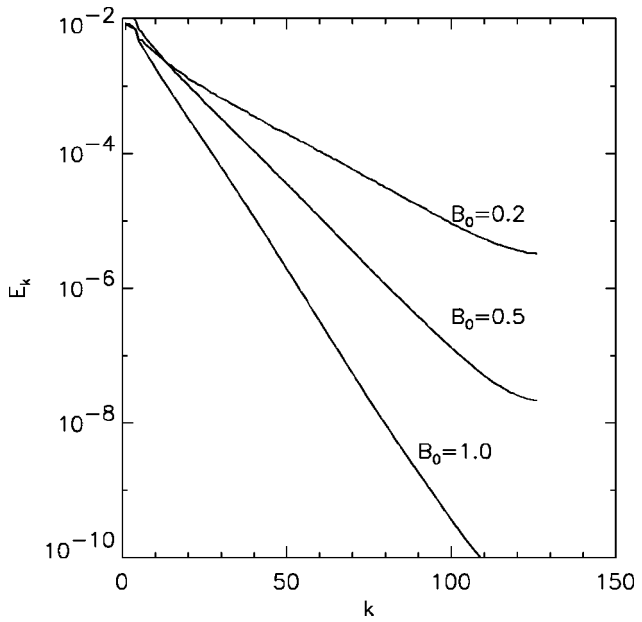


FIG. 10. Developed $E_k$ spectra for small $B_0$ RMHD solutions with initial excitation confined to $k \leqslant 4$, shown at time of peak mean parallel wave number. Spectra become approximately exponential, with a scale factor that increases with $B_0$.

and cascade. We calculate numerical solutions in this regime to test the scaling arguments of Sec. II B.

Figure 8 shows the energy in certain low- and high-$k$ modes from a $128^2 \times 256$, $B_0 = 0.2$ solution. Here, some of the initial excitation is at scales which interact only resonantly. The energy in each mode having $k > 20$ decays at a single rate. The smaller-$k$ modes decay with a different rate. We surmise, based on a similarity with Fig. 2, that as suggested in Sec. II C, there is a passive relationship between the small- and large-$k$ modes similar to the passive driving of the finite-$k$ modes by the $k = 0$ mode seen in the large-$B_0$ solutions. This relationship cannot be so simply demonstrated because of the lack of structuring in this solution. Contrary to the large-$B_0$ solutions, the $k = 0$ mode does not develop 2D-like coherent flux-tube structures. Intense, relatively short-lived current sheets do appear like those seen in 3D isotropic solutions [29], but there is no association of the current sheets with magnetic island structures as in 2D [25]. Note that because the total energy is decaying while $B_0$ is constant, $k_L$ is effectively shrinking, and the system will obey the dynamics of Sec. II A once $k_L \lesssim 1$.

If the initial conditions are such that none of the modes initially present are dominated by Alfvénic propagation, then a nonlinear cascade will transfer energy to the higher wave numbers. Because energy cannot be exchanged with modes having $k > k_L$, there is a limit imposed by $B_0$ on the extent of the cascade in $k$, as argued in Sec. II B. Figure 9 shows $\bar{k}$ and $\bar{\kappa}$ from three runs with $B_0 = 0.2$, 0.5, and 1.0 on a $128^2 \times 256$ grid. The perpendicular cascade is indifferent to the strength of $B_0$, but the parallel cascade is not. As the initial spectrum expands into higher wave numbers, the mean wave number $\bar{k}$ increases, with a maximum $\bar{k}$ that increases with decreasing $B_0$. For $B_0 = 0.2$, $\bar{k}$ peaks in the range between the active and passive modes shown in Fig. 8. After reaching its peak $\bar{k}$ does not decay as $\bar{\kappa}$ does, indicating that energy is not being dissipated by transfer to larger $k$.

Figure 10 shows the $E_k$ spectra for the same three runs as in Fig. 4 at the times of maximum $\bar{k}$. Approximately exponential spectra are evident up to the largest wave numbers, where the Fourier truncation prevents transfer to larger $k$, causing buildup at the resolution limit. Fits of the spectra to exponential curves for $20 \leqslant k \leqslant 100$ give scale factors of 16.32, 8.86, and 5.75. The ratio of these factors is 2.8:1.5:1, while the magnetic field strengths are in ratio 5:2:1. Thus the general arguments of Sec. II B give a correct order-of-magnitude estimate of the spectrum in Eq. (13), but a more careful theory is required to predict the exponential scale factor more accurately.

## IV. DISCUSSION

We have examined the effects of resonant triad interactions on broadband turbulent MHD. Under certain conditions, the cascade behavior of MHD with a strong background magnetic field is primarily determined by the resonant triad interactions in which one of the wave vectors has zero projection along the background field. When these conditions are not met, then higher-order effects will become important. In numerical solutions, we have verified quantitatively the predictions of the third-order theory and the parameter regimes in which it is no longer valid.

The third-order theory is based on a multiple-time-scale analysis, but the time scales can only be legitimately separated for parallel wave numbers greater than a characteristic parallel wave number $k_L$, defined in terms of the background field in Eq. (6). Modes with wave numbers $< k_L$ are fundamentally nonlinear and form a dynamical system of mutually interacting fields. Modes with wave number $> k_L$ (''wave modes'') are fundamentally linear and can be described by the third-order theory. They propagate nondispersively on a fast time scale, with a slowly evolving cross-sectional amplitude described by Eq. (10) for RMHD and Eq. (A9) for 3D incompressible MHD. The wave modes have no influence on the nonlinear modes.

In a system with finite extent, it is possible that even the minimum finite wave number will be greater than $k_L$. In this case, the only nonlinearly interacting mode is the one with $k = 0$, the vertically averaged field, or ''mean mode.'' Under these conditions, the only significant interactions are among resonant triads which include the mean mode. The mean mode evolves with independent 2D dynamics, and forms coherent magnetic structures which produce strong current sheets at sites of interaction. The passive dynamics of the wave modes gives them amplitudes mirroring the vortex and sheet structures of the mean mode. It is not necessary that the mean mode be energetically dominant, but its energy sets the time scale for the overall perpendicular cascade. If that time scale is very long, higher-order effects may again become important. One of the possible effects is a pumping of energy into the mean mode by the wave modes, but this question will be left for a later study.

Regardless of whether the $k < k_L$ modes are described by third-order or higher-order dynamics, all modes with wave number $> k_L$ are passive wave modes described by third-order theory. Since the energy in each individual wave mode is conserved even on the slow-time scale, there is no transfer

of energy to parallel dissipation scales. Energy is driven to perpendicular dissipation scales by the action of the $k<k_L$ modes, so an anisotropic spectrum will develop. We observe in numerical solutions that the wave modes are driven to perpendicular dissipation more rapidly than the nonlinear modes, and therefore also become weaker as $t\to\infty$.

The Kolmogorov power-law spectrum of inertial-range turbulence depends on the assumption of a scale-invariant cascade. The existence of a characteristic scale in anisotropic MHD invalidates this assumption. An interesting analogy exists with the dissipation range of Navier-Stokes turbulence. The dissipation range has a characteristic wave number, the dissipation wave number $k_d$, and energy transferred to wave numbers $>k_d$ is quickly removed from the system. In anisotropic MHD, energy transferred to parallel wave numbers $>k_L$ is decoupled from the rest of the system, even though the modes are not damped to zero. Simple scaling arguments balancing the nonlinear transfer with either viscous dissipation or the Alfvén wave restoring force suggest a spectrum which is to lowest order exponential, with scale factor proportional to the characteristic wave number, $k_d$ or $k_L$. We have shown in direct numerical solutions that such a spectrum does indeed develop.

## ACKNOWLEDGMENTS

The authors are indebted to Alexander Shchepetkin for numerical code development. This work was partially supported by the Institute of Geophysics and Planetary Physics at Los Alamos National Laboratory under Grant No. UCRP 98-823 and by the National Science Foundation under Grant No. MCA97S009N. The authors utilized the SGI Power Challenge Array at the National Center for Supercomputing Applications, University of Illinois at Urbana–Champaign.

## APPENDIX: RESONANT BEHAVIOR OF INCOMPRESSIBLE MHD

In this appendix, we show that applying the scale-dependent multiple-time-scale analysis to 3D incompressible MHD leads to the same conclusions as the RMHD analysis in the text. We denote three-dimensional vectors by an overhead arrow, to distinguish from horizontal vectors, which are denoted by boldface. We write MHD in terms of the Elsasser variables $\vec{v}\pm\vec{B}=\vec{u}^{\pm}=(\mathbf{u}^{\pm},w^{\pm})$,

$$\partial_t\vec{u}^{\pm}+\vec{u}^{\mp}\cdot\vec{\nabla}\vec{u}^{\pm}=\pm B_0\partial_z\vec{u}^{\pm}-\vec{\nabla}\pi, \tag{A1}$$

where $\pi$ is the total pressure $p+\frac{1}{2}\vec{B}\cdot\vec{B}+B_0B_z$. We consider only incompressible motions, so that $\vec{\nabla}\cdot\vec{u}^{\pm}=0$, and

$$(\vec{\nabla}\cdot\vec{\nabla})\,\pi=-\vec{\nabla}\cdot(\vec{u}^{\mp}\cdot\vec{\nabla}\vec{u}^{\pm}). \tag{A2}$$

The important point is that $\pi$ does not scale like $B_0$, but with the fluctuations $\vec{u}^{\pm}$.

The equations for the perpendicular and parallel components are

$$\partial_t\mathbf{u}^{\pm}+\mathbf{u}^{\mp}\cdot\boldsymbol{\nabla}\mathbf{u}^{\pm}+\mathbf{u}^{\pm}(\boldsymbol{\nabla}\cdot\mathbf{u}^{\pm})+\boldsymbol{\nabla}\pi=\partial_z[\pm B_0\mathbf{u}^{\pm}-w^{\mp}\mathbf{u}^{\pm}], \tag{A3}$$

$$\partial_t w^{\pm}+\mathbf{u}^{\mp}\cdot\boldsymbol{\nabla}w^{\pm}+w^{\pm}(\boldsymbol{\nabla}\cdot\mathbf{u}^{\mp})+\partial_z\pi=\partial_z[\pm B_0w^{\pm}-w^{\mp}w^{\pm}]. \tag{A4}$$

Writing again in terms of the vertical Fourier components, we have

$$\partial_t\mathbf{u}_k^{\pm}+\sum_{k'}\,[\mathbf{u}_{k'}^{\mp}\cdot\boldsymbol{\nabla}\mathbf{u}_{k-k'}^{\pm}+\mathbf{u}_{k-k'}^{\pm}(\boldsymbol{\nabla}\cdot\mathbf{u}_{k'}^{\mp})]+\boldsymbol{\nabla}\pi_k=ik\left[\pm B_0\mathbf{u}_k^{\pm}-\sum_{k'}\,w_{k'}^{\mp}\mathbf{u}_{k-k'}^{\pm}\right], \tag{A5}$$

$$\partial_t w_k^{\pm}+\sum_{k'}\,[\mathbf{u}_{k'}^{\mp}\cdot\boldsymbol{\nabla}w_{k-k'}^{\pm}+w_{k-k'}^{\pm}(\boldsymbol{\nabla}\cdot\mathbf{u}_{k'}^{\mp})]+ik\pi_k=ik\left[\pm B_0w_k^{\pm}-\sum_{k'}\,w_{k'}^{\mp}w_{k-k'}^{\pm}\right]. \tag{A6}$$

Provided that

$$B_0\gg w_k^{\pm},\forall k \tag{A7}$$

i.e., that the mean vertical field is larger than the parallel fluctuations, the linear terms on the right hand side will be dominant over the nonlinear terms for $k$ greater than some finite value $k_L\sim|\boldsymbol{\nabla}u^{\pm}|/B_0$. If $k_L$ is smaller than the occupied wave numbers of the system, we can split the time variable into fast- and slow-time scale, $t'$ and $\tau$, and find

$$\partial_{t'}\mathbf{u}_k^{\pm}=\pm ikB_0\mathbf{u}_k^{\pm},$$

$$\partial_{t'}w_k^{\pm}=\pm ikB_0w_k^{\pm}. \tag{A8}$$

The divergence-free parts of the $\mathbf{u}$ oscillations are shear Alfvén waves, while the $w^{\pm}$ oscillations are ''pseudo-Alfvén'' waves, which are actually the incompressible remnants of the fast magnetosonic mode. In fact, pseudo-Alfvén waves are strongly damped by kinetic effects [30], but we retain them here for generality.

Just as in the RMHD case, when averaging over $t'$ to obtain the slow-time-scale behavior, only the $k'=0$ terms contribute. Since $\boldsymbol{\nabla}\cdot\mathbf{u}_{k=0}^{\pm}=0$, we may write $\mathbf{u}_{k=0}^{\pm}=\hat{\mathbf{z}}\times\boldsymbol{\nabla}\psi_0^{\pm}$. The result for the slow-time-scale evolution of the Fourier amplitudes is

$$\partial_\tau\mathbf{u}_k^{\pm}+[\psi_0^{\mp},\mathbf{u}_k^{\pm}]=-ikw_0^{\mp}\mathbf{u}_k^{\pm}-\boldsymbol{\nabla}\overline{\pi}_k,$$

$$\partial_\tau w_k^{\pm}+[\psi_0^{\mp},w_k^{\pm}]=-ikw_0^{\mp}w_k^{\pm}-ik\overline{\pi}_k,$$

$$\boldsymbol{\nabla}\cdot\mathbf{u}_k^{\pm}+ikw_k^{\pm}=0. \tag{A9}$$

The time-averaged total pressure $\overline{\pi}_k$ assures incompressibility and depends only on $\vec{u}_0^{\pm}$ and $\vec{u}_k^{\pm}$. The RMHD result of Sec. II A is obtained by taking $w_k=0$ and writing $\mathbf{u}_k=\hat{\mathbf{z}}\times\boldsymbol{\nabla}\psi_k^{\pm}$.

The fundamental result is that the only independently evolving mode is the $k=0$ mean mode, and the finite-$k$ modes are driven by the mean mode, with $\int|\mathbf{u}_k^{\pm}|^2+\int|w_k^{\pm}|^2d\mathbf{x}$ conserved individually for each $k$. Therefore the total energy in each mode is invariant, and no parallel

cascade occurs on either the fast- or the slow-time scale. The conclusion is similar to that based on analysis of RMHD in the text, but is more general because here we have not assumed any relative scaling of the perpendicular and parallel component amplitudes or length scales. Rather than the simple scalar dynamics of Eq. (10), each mode has $\mathbf{u}_k^{\pm}$ and $w_k^{\pm}$ dynamics. It should also be noted that the parallel components of the mean mode, $w_0^{\pm}$, are nonzero but passively driven by $\psi_0^{\pm}$. Since our numerical solutions indicate that passive fields are more rapidly driven to perpendicular dissipation scales, the long-time state of the system will be one in which both the finite-$k$ modes and the $w_0^{\pm}$ components have been removed.


[1] D. A. Frail, P. J. Diamond, J. M. Cordes, and H. J. van Langevelde, Astrophys. J. Lett. **427**, L43 (1994).
[2] J. W. Armstrong, W. A. Coles, M. Kojima, and B. J. Rickett, Astrophys. J. **358**, 685 (1990).
[3] W. H. Matthaeus, M. L. Goldstein, and D. A. Roberts, J. Geophys. Res. **95**, 20 673 (1990).
[4] J. W. Belcher and L. Davis, Jr., J. Geophys. Res. **76**, 3534 (1971).
[5] L. Klein, D. A. Roberts, and M. L. Goldstein, J. Geophys. Res. **96**, 3779 (1991).
[6] S. Zweben, C. Menyuk, and R. Taylor, Phys. Rev. Lett. **42**, 1270 (1979).
[7] S. Oughton, E. R. Priest, and W. H. Matthaeus, J. Fluid Mech. **280**, 95 (1994).
[8] W. H. Matthaeus, S. Ghosh, S. Oughton, and D. A. Roberts, J. Geophys. Res. **101**, 7619 (1996).
[9] A. Pouquet, U. Frisch, and J. Léorat, J. Fluid Mech. **77**, 321 (1976).
[10] R. H. Kraichnan, Phys. Fluids **8**, 1385 (1965).
[11] R. S. Iroshnikov, Astron. Zh. **40**, 742 (1963).
[12] J. V. Shebalin, W. H. Matthaeus, and D. Montgomery, J. Plasma Phys. **29**, 525 (1983).
[13] D. Montgomery and W. H. Matthaeus, Astrophys. J. **447**, 706 (1995).
[14] S. Sridhar and P. Goldreich, Astrophys. J. **432**, 612 (1994).
[15] P. Goldreich and S. Sridhar, Astrophys. J. **438**, 763 (1995).
[16] B. B. Kadomtsev, *Plasma Turbulence* (Academic, New York, 1965).
[17] H.-O. Kreis, Commun. Pure Appl. Math. **33**, 399 (1980).
[18] C. S. Ng and A. Bhattacharjee, Astrophys. J. **465**, 845 (1996).
[19] P. Goldreich and S. Sridhar, Astrophys. J. **485**, 680 (1997).
[20] H. R. Strauss, Phys. Fluids **19**, 134 (1976).
[21] D. Montgomery, Phys. Scr. **T2/1**, 93 (1982).
[22] R. Kinney and J. C. McWilliams, J. Plasma Phys. **57**, 93 (1997).
[23] D. Montgomery and L. Turner, Phys. Fluids **24**, 825 (1981).
[24] G. P. Zank and W. H. Matthaeus, J. Plasma Phys. **48**, 85 (1992).
[25] R. Kinney, J. C. McWilliams, and T. Tajima, Phys. Plasmas **2**, 3623 (1995).
[26] S. I. Braginskii, Rev. Plasma Phys. **1**, 205 (1965).
[27] A. Shchepetkin and J. C. McWilliams, Mon. Weather Rev. (to be published).
[28] J. C. McWilliams, Phys. Fluids A **2**, 547 (1990).
[29] H. Politano, A. Pouquet, and P. L. Sulem, Phys. Plasmas **2**, 2931 (1995).
[30] A. Barnes, Phys. Fluids **9**, 1483 (1966).